Selective recognition of tetrahedral dianions by a hexaaza cryptand receptor†

Pedro Mateus,[a] Rita Delgado,*[a,b] Paula Brandão,[c] Sílvia Carvalho[d] and Vítor Félix[d]

Received 30th June 2009, Accepted 4th August 2009
First published as an Advance Article on the web 9th September 2009
DOI: 10.1039/b912940e

A hexaamine cage was synthesised in good yield by a [2+3] Schiff-base condensation followed by sodium borohydride reduction to be used as a receptor for the selective binding of anionic species. The protonation constants of the receptor, as well as its association constants with Cl^-, I^-, NO_3^-, AcO^-, ClO_4^-, $H_2PO_4^-$, SO_4^{2-}, SeO_4^{2-} and $S_2O_3^{2-}$ were determined by potentiometry at 298.2 ± 0.1 K in H_2O–MeOH (50 : 50 v/v) and at ionic strength 0.10 ± 0.01 mol dm^{-3} in KTsO. These studies revealed a remarkable selectivity for dianionic tetrahedral anions by the protonated receptor, with association constants ranging 5.03–5.30 log units for the dianionic species and 1.49–2.97 log units for monoanionic ones. Single crystal X-ray determination of $[(H_6xyl)(SO_4)(H_2O)_6](SO_4)_2{\cdot}9.5H_2O$ showed that one sulfate anion is encapsulated into the receptor cage sited between the two 2,4,6-triethylbenzene caps establishing three N–H ⋯ O hydrogen bonds with two adjacent N–H binding sites and additional O–H ⋯ O hydrogen bonding interactions with six water of crystallization molecules. Four water molecules of the $(SO_4)(H_2O)_6$ cluster interact with $[H_6xyl]^{6+}$ through N–H ⋯ O hydrogen bonds. Molecular dynamics simulations (MD) carried out with SO_4^{2-} and Cl^- anions in H_2O–MeOH (50 : 50 v/v) allowed the full understanding of anion molecular recognition, the selectivity of the protonated receptor for SO_4^{2-} and the role played by the methanol and water solvent molecules.

Introduction

Achieving selective recognition, strong binding and transport of anions by synthetic receptors is a goal pursued by many researchers working in the supramolecular chemistry field, as a variety of potential applications can be devised in biomedical and environmental areas.[1] For instance, it as been pointed out that the disease cystic fibrosis is related to a dysfunction of chloride channels and that phosphate and sulfate homeostasis is difficult to maintain in chronic renal disease patients.[2,3] Moreover, the removal of anionic pollutants such as nitrate and phosphate from waterways, the treatment of wastewaters containing toxic anions (pertechnetate, arsenate, selenate and chromate) and the removal of sulfate from nitrate rich nuclear wastes are also desirable developments.[4]

Despite the considerable effort put into the design of new synthetic receptors, the task of achieving high affinity and selectivity in aqueous media has been quite challenging due to the intrinsic characteristics of anions (larger sizes as compared to isoelectronic metal ions, their variety of shapes, high hydration energy and pH dependency), and of the receptor that may not be able to confer the necessary rigidity and complementarity for the recognition of the partner. In fact, if the receptor is flexible enough to adapt to the stereochemical requirements of the substrate by distorting its structure or rearranging its conformation, it loses selectivity.

Bearing this in mind we decided to take advantage of the well known ability of tren [tris(2-aminoethyl)amine] derived polyammonium cryptands to strongly bind anions in aqueous media by combining electrostatic and hydrogen bonding interactions,[5] aiming to obtain a more rigid structure by using 2,4,6-triethylbenzenes as caps instead of tren. In addition we also expect that the 2,4,6-triethylbenzene capped cryptands will be more lipophilic than the tren derived ones, a characteristic of importance for extraction and transport applications.[6] Therefore, a receptor with *m*-xylyl groups as spacers was synthesised and its binding ability to encapsulate anions of different shape, size and charge was investigated.

Although tren derived polyammonium cryptands have been extensively studied as receptors for anions, the benzene capped analogs are practically unexplored. In fact, besides an early article by Lehn and Heyer describing the synthesis and anion binding properties of two benzene capped polyammonium cryptands with aliphatic spacers,[7] only one such cryptand has been reported so far but has been explored for its carbohydrate recognition rather than for anion recognition.[8] It was not until very recently, and when our studies were in progress, that an almost identical cryptand was studied as a halide receptor in DMSO-d_6 by ^{1}H-NMR spectroscopy, although no quantitative binding information was supplied.[9]

[a]*Instituto de Tecnologia Química e Biológica, UNL, Av. da República – EAN, 2780-157 Oeiras, Portugal. E-mail: delgado@itqb.unl.pt; Fax: (+351) 21 441 12 77*
[b]*Instituto Superior Técnico, DEQB, Av. Rovisco Pais, 1049-001 Lisboa, Portugal*
[c]*Departamento de Química, CICECO, Universidade de Aveiro, 3810-193 Aveiro, Portugal*
[d]*Departamento de Química, CICECO and Secção Autónoma de Ciências da Saúde, Universidade de Aveiro, 3810-193 Aveiro, Portugal. E-mail: vitor.felix@ua.pt*

† Electronic supplementary information (ESI) available: NMR and mass spectra, simulation results and anion protonation constants. CCDC 734450. For ESI and crystallographic data in CIF or other electronic format see DOI: 10.1039/b912940e

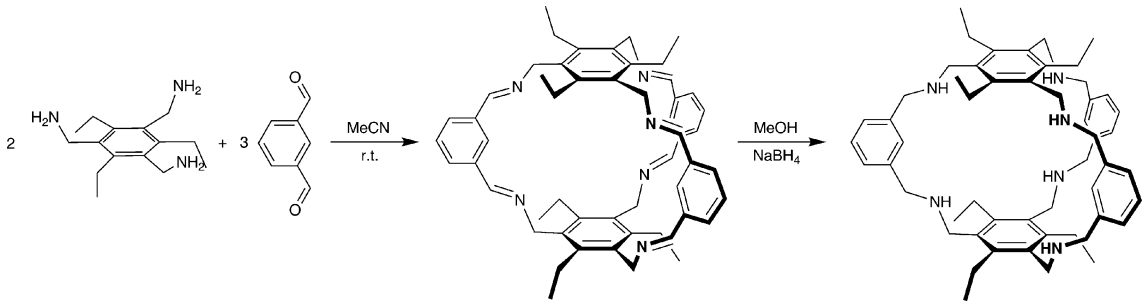

Scheme 1 Synthetic procedure to xyl.

Results and discussion

Synthesis of the cryptand

The cryptand was prepared through a modification of the general synthetic method reported by Chen and Martell,[10] as outlined in Scheme 1. Reaction between 1,3,5-tris(aminomethyl)-2,4,6-triethylbenzene and isophthaldehyde in a 2 : 3 ratio in MeCN, yielded the desired hexaimine cage in surprisingly good yield, taking into account the simultaneous formation of six bonds. The preorganization of both caps and spacers greatly facilitated the synthesis: the alternating substitution pattern in 1,3,5-tris(aminomethyl)-2,4,6-triethylbenzene ensures that the amine groups are oriented on the same face of the aromatic ring[11] while the *meta* positions of the carbonyl groups in isophthaldehyde provide the right angle for the mutual complementarity of the reagents. We found that under the same conditions, the reactions of 1,3,5-tris(aminomethyl)benzene with isophthaldehyde and of 1,3,5-tris(aminomethyl)-2,4,6-triethylbenzene with terephthalaldehyde gave mostly insoluble polymeric materials and less than 5% of the desired hexaimines. Reduction of the hexaimines with $NaBH_4$ resulted in the corresponding hexaamines.

Potentiometric studies: acid–base behaviour

The choice of an appropriate background electrolyte to maintain the ionic strength was the first decision to take before the potentiometric measurements for the determination of protonation or association constants were undertaken. The electrolyte salt cannot contain anions that may interact with the receptor, because it is present in very large concentration compared to the receptor and the substrate species. The bulky potassium tosylate (KTsO) was chosen based on the assumption that it does not appreciably interact with the receptor, as also observed for the tren-capped cryptands.[5b,e,7,12] The determined constants are conditional values that hold only for the specific medium used.

The determination of the protonation constants of xyl and all the studied substrates alone and in the same medium was the next step. The measurements were carried out at 298.2 ± 0.1 K in H_2O–MeOH (50 : 50 v/v) and at ionic strength 0.10 ± 0.01 mol dm^{-3} in KTsO, and the results are shown in Table 1 and Table S1 (see ESI†).

The first protonation constant of xyl could not be accurately determined due to precipitation at pH 7.75. Thus the value was estimated at 8.7, assuming that the difference between the first and second protonation constants is mainly due to both statistical factors and electrostatic repulsions. Taking this into account, six protonation constants were found for the xyl cryptand in the working pH region (2.90–7.75) corresponding to the successive protonation of the secondary amines, with the values decreasing steadily with increasing protonation state due to the build up of positive charges. The corresponding species distribution diagram, represented in Fig. 1, shows that the hexaprotonated form, H_6xyl^{6+}, exists as the main species up to a pH of about 4.5, at which value all the studied substrates are deprotonated, except dihydrogen phosphate and acetate anions.

Table 1 Overall (β_i^H) and stepwise protonation (K_i^H) constants of xyl in H_2O–MeOH (50 : 50 v/v); $T = 298.2 \pm 0.1$ K; $I = 0.10 \pm 0.01$ mol dm^{-3} in KTsO

Equilibrium reaction	log β_i^H[a]	Equilibrium reaction	log K_i^H
$xyl + H^+ \rightleftharpoons Hxyl^+$	8.7[b]	$xyl + H^+ \rightleftharpoons Hxyl^+$	8.7
$xyl + 2H^+ \rightleftharpoons H_2xyl^{2+}$	16.56(1)	$Hxyl^+ + H^+ \rightleftharpoons H_2xyl^{2+}$	7.86
$xyl + 3H^+ \rightleftharpoons H_3xyl^{3+}$	23.77(1)	$H_2xyl^{2+} + H^+ \rightleftharpoons H_3xyl^{3+}$	7.21
$xyl + 4H^+ \rightleftharpoons H_4xyl^{4+}$	30.32(1)	$H_3xyl^{3+} + H^+ \rightleftharpoons H_4xyl^{4+}$	6.55
$xyl + 5H^+ \rightleftharpoons H_5xyl^{5+}$	36.29(1)	$H_4xyl^{4+} + H^+ \rightleftharpoons H_5xyl^{5+}$	5.97
$xyl + 6H^+ \rightleftharpoons H_6xyl^{6+}$	41.28(1)	$H_5xyl^{5+} + H^+ \rightleftharpoons H_6xyl^{6+}$	4.99

[a] Values in parentheses are standard deviations in the last significant figures. [b] Estimated value, see text.

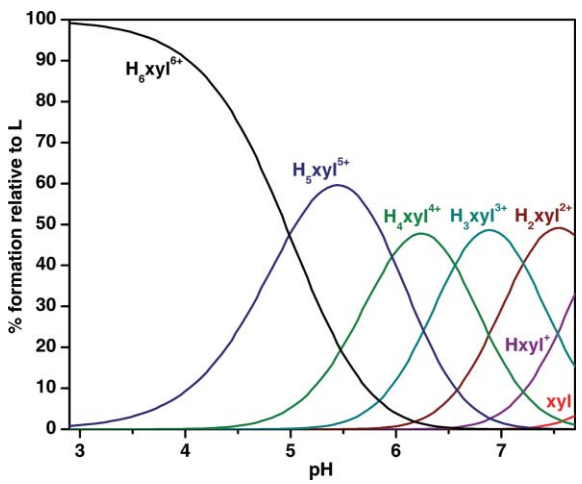

Fig. 1 Species distribution diagram for the protonation of xyl. $C_{xyl} = 1 \times 10^{-3}$ mol dm^{-3}.

The overall basicity of the receptor is lower than expected for secondary amines due to the electron withdrawing effect of the *m*-xylyl rings and the 2,4,6-triethylbenzene caps. Indeed the tren derived cryptand with *m*-xylyl spacers[5f] is more basic than xyl in

Table 2 Overall ($\log \beta_{H_bL_lA_a}$)[a] and stepwise ($\log K_{H_bL_lA_a}$) association constants for the indicated equilibria[b] in H_2O–MeOH (50 : 50 v/v); $T = 298.2 \pm 0.1$ K; $I = 0.10 \pm 0.01$ mol dm^{-3} in KTsO

Equilibrium	Cl^-	I^-	NO_3^-	ClO_4^-	AcO^-	SO_4^{2-}	SeO_4^{2-}	$S_2O_3^{2-}$	HPO_4^{2-}
$7H^+ + L + A \rightleftharpoons H_7LA$	—	—	—	—	—	—	—	—	50.86(5)
$6H^+ + L + A \rightleftharpoons H_6LA$	43.29(4)	42.77(7)	43.33(4)	43.07(6)	38.57(2)	46.31(1)	46.32(1)	46.58(1)	46.72(2)
$5H^+ + L + A \rightleftharpoons H_5LA$	—	—	—	—	32.52(3)	40.03(1)	40.13(1)	40.36(1)	40.41(2)
$4H^+ + L + A \rightleftharpoons H_4LA$	—	—	—	—	26.03(3)	33.01(3)	33.00(1)	33.12(3)	33.66(2)
$3H^+ + L + A \rightleftharpoons H_3LA$	—	—	—	—	18.86(4)	—	—	—	—
$2H^+ + L + A \rightleftharpoons H_2LA$	—	—	—	—	10.8(1)	—	—	—	—
				Stepwise constants					
$H_6L^{6+} + A' \rightleftharpoons H_6LA'$	2.01	1.49	2.05	1.79	—	5.03	5.04	5.30	2.12
$H_5L^{5+} + A' \rightleftharpoons H_5LA'$	—	—	—	—	2.28	3.74	3.84	4.07	2.97
$H_4L^{4+} + A' \rightleftharpoons H_4LA'$	—	—	—	—	2.20	2.69	2.67	2.80	2.63
$H_3L^{3+} + A' \rightleftharpoons H_3LA'$	—	—	—	—	2.27	—	—	—	2.43
$H_2L^{2+} + A' \rightleftharpoons H_2LA'$	—	—	—	—	2.30	—	—	—	—
$HL^+ + A' \rightleftharpoons HLA'$	—	—	—	—	2.1	—	—	—	—

[a] Values in parentheses are standard deviations for the last significant figure. [b] L = xyl, A = Cl^-, I^-, NO_3^-, ClO_4^-, AcO^-, SO_4^{2-}, SeO_4^{2-}, $S_2O_3^{2-}$ and HPO_4^{2-} (because only $H_2PO_4^-$ and HPO_4^{2-} are important in the pH range studied this anion was considered diprotic), A′ = A in all cases except for phosphate where A′ = $H_2PO_4^-$. Charges were omitted in species involving A for simplicity.

each protonation step and the related cryptand with five –CH_2– groups bridging the two tren caps[5c] is the most basic one.

Potentiometric studies: binding affinities

The association constants of the protonated forms of xyl with several anions differing in shape, size and charge were determined in H_2O–MeOH (50 : 50 v/v) solutions at 298.2 K and 0.10 mol dm^{-3} KTsO. The values obtained are collected in Table 2.

A better way to visualise the affinity of the receptor for each anion along the pH region is provided by plots of the effective association constant (Fig. 2), K_{eff}, as a function of the pH. The K_{eff} value is defined as the quotient between the total amount of supramolecular species formed and the total amounts of the free receptor and free substrate: $K_{eff} = \Sigma[H_{i+j}AR]/\Sigma[H_iA]\times\Sigma[H_jR]$.[13] This value takes into consideration the different basicities of receptors and substrates and thus provides a suitable way to derive selectivity trends. Furthermore, whenever there are overlapping protonation equilibria between receptors and anions, it is possible to distinguish the stepwise equilibria that effectively occur from all those that can be established for each case.

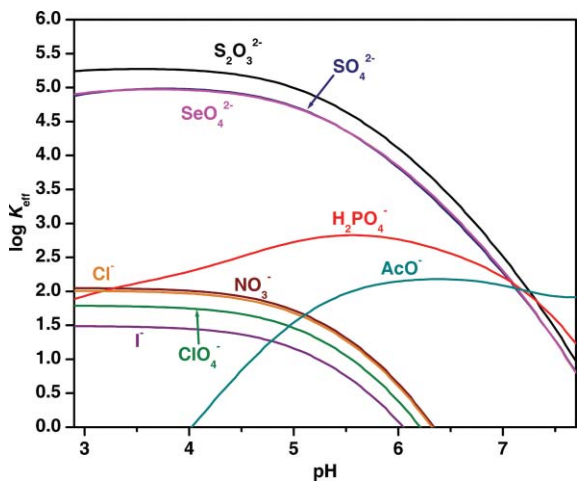

Fig. 2 Plots of the effective association constant K_{eff} (in log units) *versus* pH for the supramolecular species formed between protonated xyl and the anions studied. $C_{xyl} = C_A = 1 \times 10^{-3}$ mol dm^{-3}.

Only species of 1 : 1 (receptor to anionic substrate) stoichiometry were found for all the cases and at different protonation states of xyl. As expected, the association constants increase with increasing positive charge on the receptor and increasing negative charge on the anionic substrate, suggesting that the main interactions are electrostatic in nature, although contributions due to hydrogen bonding are not to be ruled out. In fact, the mononegative and poor hydrogen bond acceptor anions, I^- and ClO_4^-, have the lowest association constants.

Due to the pK_a value of acetate, there is no interaction between this anion and the fully protonated receptor. Furthermore, the association constants do not vary appreciably with decreasing protonation of the receptor. This indicates that acetate is bound to the receptor by only one or two donor centres.

The binding constant of dihydrogen phosphate with H_6xyl^{6+} is smaller than that with H_5xyl^{5+}. This probably is due to the fact that in the pH region where these species are formed, the H_6xyl^{6+} species coexists in solution partly with H_3PO_4 and H_6xyl^{6+} has no hydrogen bond acceptors to interact with the protons of the substrate. On the other hand, in the H_5xyl^{5+} form, one of the amines can act as a hydrogen bond acceptor of the OH groups in dihydrogen phosphate, which accounts for the larger constant. However, because the interactions are mainly electrostatic in nature, the association constants progressively drop with the decrease of protonation state of the receptor, although to a lesser extent than in the cases of sulfate, selenate and thiosulfate, indicating that the hydrogen bond donating/accepting abilities of dihydrogen phosphate are still playing a role. This behaviour somewhat recalls the sulfate-binding protein, as its low affinity to phosphate is mainly attributed to the lack of hydrogen bond acceptors in the binding site.[14]

However, the most interesting point of the behaviour of the receptor under study is its remarkable selectivity for dinegative anions over mononegative ones, although the receptor fails to discriminate between anionic substrates of the same charge and shape. Selenate and sulfate exhibit the same binding affinities, within experimental error, whereas thiosulfate is the most strongly

bound. Although the mean S–O distance in thiosulfate should be comparable to that of sulfate and selenate, the long S–S bond and the larger radius of the sulfur atom should account for the enhanced binding constant. This has been found to be true in the crystal structure of the tren derived analog with *m*-xylyl spacers in which thiosulfate is the only anion that is able to bind directly to all six protonated amines *via* hydrogen bonds.[15]

The remarkable high selectivity of the receptor for dinegative anions over all mononegative anions studied can be better visualised by a competitive binding diagram, in which the overall percentages of the associated species as a function of pH are displayed for systems containing the receptor and several anions in equimolar amounts.[16] It is quite clear in Fig. 3 that at pH values below 5 the receptor binds exclusively to sulfate in a mixture of equimolar amounts of chloride, iodide, nitrate, perchlorate, dihydrogen phosphate and acetate.

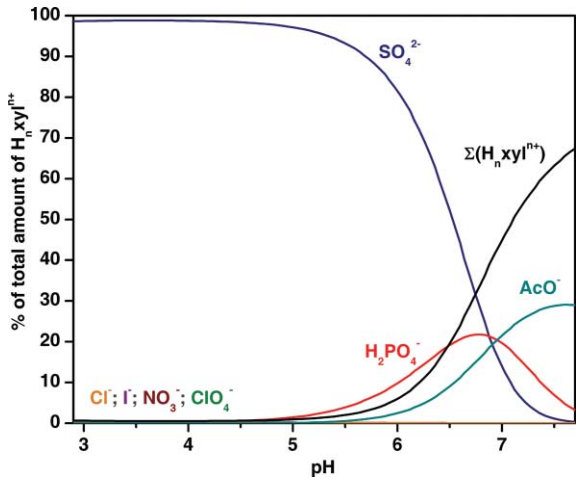

Fig. 3 Distribution diagram of the overall amounts of supramolecular species formed between the receptor, H_nxyl^{n+}, and each anion. Where SO_4^{2-}, $H_2PO_4^-$, AcO^-, Cl^-, I^-, NO_3^- and ClO_4^- represent $\sum[(H_nxyl)(A)]$, A being the indicated anion. $C_{xyl} = C_{anion}/3 = 1 \times 10^{-3}$ mol dm^{-3}.

NMR studies

The ^{1}H NMR spectra of xyl were acquired in D_2O at pD = 3.80 and 298.2 K, see Fig. 4. At this pD value the receptor is expected to be completely protonated (see Fig. 1). The number and integration of the signals observed in the ^{1}H NMR spectra of H_6xyl^{6+} suggest a highly symmetric structure in solution, consistent with the presence of a C_3 symmetry axis and a horizontal symmetry plane. Another interesting feature is that the tosylate resonances in $H_6xyl(TsO)_6$ are shifted upfield in relation to their free form at the same pD. Moreover, the biggest shift is observed for the doublet resonance corresponding to the hydrogen atoms in the *ortho* position relative to the sulfonate group, while the doublet assigned to the ones in the *meta* position is less shifted and the methyl hydrogen atoms have almost no shift. This indicates that the sulfonate groups are at the entrance of the cavity, with the methyl groups pointing outwards, suggesting that the tosylate is bound in a cleft manner, most likely interacting with the protonated amines that should, on the other hand, be turned outside the cavity. These observations are in close agreement with the reported

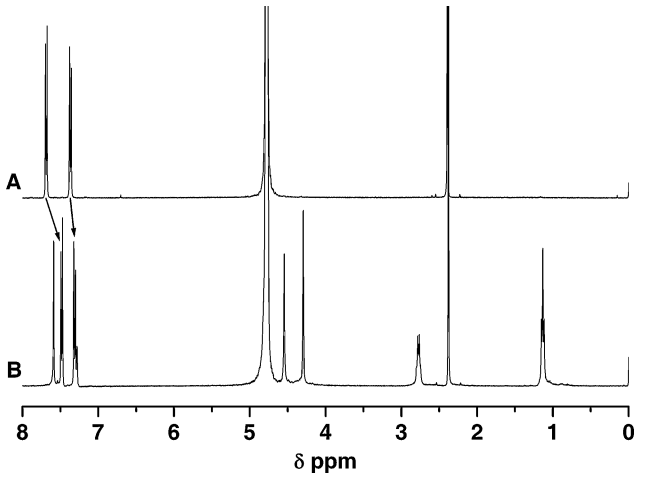

Fig. 4 ^{1}H NMR spectra of KTsO (A) and of $H_6xyl(TsO)_6$ (B) in D_2O at pD = 3.80 and 298.2 K.

crystal structure of the hexaprotonated tren derived analog with *m*-xylyl spacers, having tosylate as counterion.[12c]

The ^{1}H-NMR spectra of solutions of equimolar amounts of the receptor and the anionic substrates in D_2O at pD = 3.80 were also recorded (see Fig. S8, ESI†). In all cases, only one set of signals was observed for the free receptor and for the associated entities, indicating fast receptor–substrate exchanges on the NMR time scale. As shown in Fig. S8 (see ESI†), in these conditions the shifts of resonances are significant only for sulfate.

The stoichiometry of the H_6xyl^{6+}–SO_4^{2-} associated species was confirmed by preparing a Job's plot[17] in which the induced shift was plotted against the mole fraction of the receptor. One-to-one binding was indicated by the maximum value at the host mole fraction of 0.5 (Fig. 5).

The set of spectra obtained for the Job's plot also carried additional structural information on the binding event. First of all, it is very clear that the tosylate is excluded from the proximity of the receptor in the presence of sulfate, as its chemical shift values tend to those of the free tosylate as the amount of sulfate increases. Furthermore, except for the small upfield shift of the benzylic protons **c**, no significant shifts were observed for protons related to the caps, namely, protons **a** and **b**, indicating that, as expected, the caps function as rigid scaffolds and that the binding event affects mostly the spacers. In this regard, it can be seen that the proton resonances **d** and **g** undergo the biggest shifts. Surprisingly, downfield shifts are observed for these two protons, which could be attributable to a rearrangement of the receptor upon binding, probably the rotation of the protonated amines to the inside of the cavity. All these observations strongly suggest that the sulfate anion is encapsulated within the receptor cavity.

Electrospray mass spectrometry studies on sulfate cryptate

The ESI mass spectra acquired in positive polarity mode using solutions of 1 : 1 receptor to sulfate stoichiometry in H_2O–MeOH (50 : 50 v/v) at pH 3.80 (Fig. 6), showed peaks corresponding to the free receptor and to the sulfate cryptate. Only one species formed between the association of the hexaprotonated xyl and sulfate was found, $[(H_6xyl)(TsO)_2(SO_4)]^{2+}$ at m/z 624.3, along with two other peaks at m/z 661.3 and 441.1, corresponding to

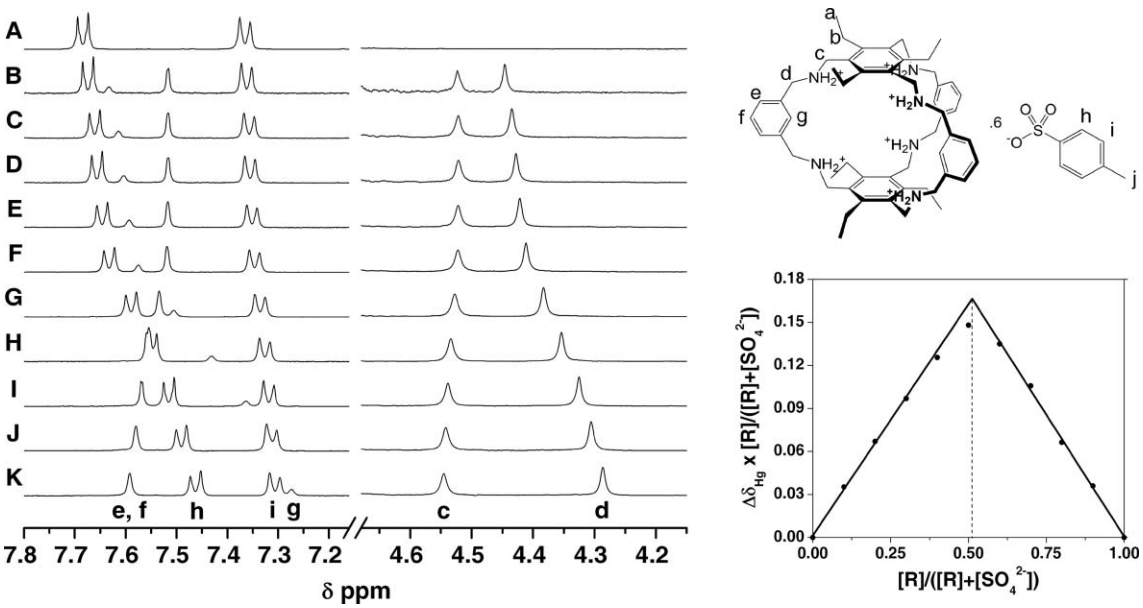

Fig. 5 Job's plot between H_6xyl^{6+} (R) and sulfate in D_2O at pD = 3.80 and 298.2 K. X = [R]/([R]+[SO_4^{2-}]), being in each spectrum the amount of X: 0 (A), 0.1 (B), 0.2 (C), 0.3 (D), 0.4 (E), 0.5 (F), 0.6 (G), 0.7 (H), 0.8 (I), 0.9 (J), and 1.0 (K), respectively. In all the recorded spectra [R] + [SO_4^{2-}] = 2×10^{-3} mol dm^{-3}. Changes of chemical shifts of the H_g resonance in the receptor were monitored (lower right corner).

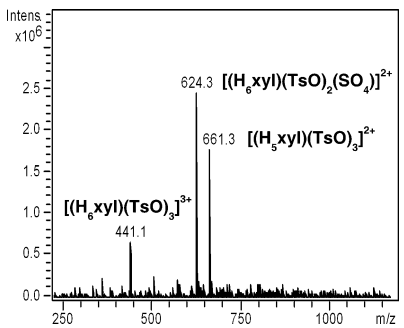

Fig. 6 ESI mass spectrum of a solution of 1 : 1 receptor to sulfate stoichiometry in H_2O–MeOH (50 : 50 v/v) at pH = 3.80.

penta- and hexaprotonated species of the free receptor, $[(H_5xyl)(TsO)_3]^{2+}$ and $[(H_6xyl)(TsO)_3]^{3+}$, respectively. These results are in agreement with the potentiometric and ^{1}H-NMR studies, where the hexaprotonated species give rise to more stable cryptates and the binding stoichiometry is 1 : 1. In a competition experiment using a solution of 1 : 1 : 1 receptor/sulfate/nitrate stoichiometry in H_2O–MeOH (50 : 50 v/v) at pH 3.80 (Fig. S10, in ESI†) the spectrum is identical to the one obtained with solutions of 1 : 1 receptor to sulfate stoichiometry, demonstrating the high sulfate/nitrate selectivity.

Crystallographic studies

The crystal structure of the sulfate cryptate is built from an asymmetric unit composed of H_6xyl^{6+} hexaprotonated receptor, three sulfate anions and sixteen water molecules, one of them with half occupancy, which is consistent with the molecular formula $[(H_6xyl)(SO_4)(H_2O)_6](SO_4)_2 \cdot 9.5H_2O$. One sulfate anion is entirely encapsulated into the macrobicyclic cage as shown in Fig. 7 in two different views, (a) and (b). The sulfate anion is sited between the

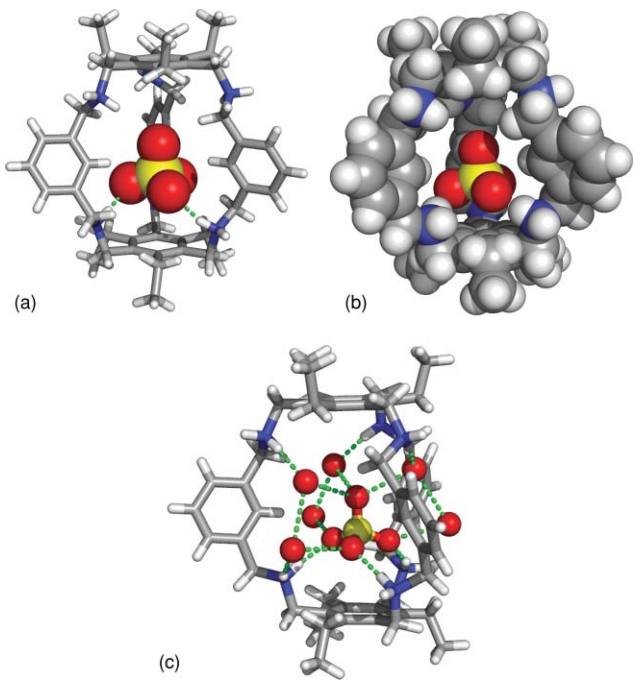

Fig. 7 Perspective views illustrating different structural features in the associated entity formed between SO_4^{2-} and the H_6xyl^{6+} receptor: (a) view showing the sulfate anion inserted into the receptor cavity and its relative position to the two 2,4,6-triethylbenzene rings; (b) space-filling view emphasizing the complete encapsulation of sulfate into the cage; (c) hydrogen bonding interactions of the $(SO_4)(H_2O)_6$ cluster with receptor N–H binding centres. The disordered water molecule is shown only in one position. Sulfur, carbon, nitrogen, hydrogen and oxygen atoms are shown in yellow, gray, blue, white and red, respectively. N–H ··· O hydrogen bonds are drawn as green dashed lines.

two 2,4,6-triethylbenzene caps at 1.109 Å from the mass centre of the cage determined by the six nitrogen atoms, leading to distances between the centroids of the 2,4,6-triethylbenzene rings and the sulfur atom of 5.540 and 3.604 Å, Fig. 7(a). Accordingly, the SO_4^{2-} anion establishes only three straight N–H···O hydrogen bonds with two adjacent N–H binding sites at N···O distances of 2.810, 2.847 and 2.943 Å and N–H···O corresponding angles of 167, 175 and 152°, respectively. Furthermore, the perspective view presented in Fig. 7(c) indicates that the sulfate anion is also assembled with six water of crystallization molecules on a network of O–H···O hydrogen bonding interactions with $O_{water}\cdots O_{sulfate}$ distances ranging from 2.715 to 2.868 Å and $O_{water}\cdots O_{water}$ distances of 2.935 and 2.905 Å. Four water molecules of the $(SO_4)(H_2O)_6$ cluster interact with H_6xyl^{6+} through N–H···O hydrogen bonds with N···O distances between 2.819 and 2.953 Å. In other words, the molecular recognition of the sulfate anion involves multiple and cooperative N–H···O and O–H···O hydrogen bonding interactions. Another interesting feature revealed by Fig. 7(a) and 7(b) is that the 2,4,6-triethylbenzene substituents are positioned above the corresponding arene rings, leaving the binding pocket unlocked for the sulfate entrance.

The H_6xyl^{6+} receptor displays an almost C_3 symmetry, see Fig. 7(b) with a 3-fold axis perpendicular to the two parallel 2,4,6-triethylbenzene ring caps with lines determined by the centroids of the *m*-xylyl spacers and the mass centre of the cage intercepting at α angles of 120.0, 122.2 and 117.7°. Comparable binding arrangements were found in the cryptates of the hexaprotonated related 2,4,6-trimethylbenzene-capped hexaazacryptand with *m*-xylyl spacers with iodide and $Cl_3(H_2O)_5$ cluster recently reported.[9] In the first case, the iodide is also inside the cryptand cage as well as disordered water bounded in a cleft fashion, while in the $Cl_3(H_2O)_5$ cryptate only two water molecules of the cluster are inside the pocket. The intramolecular distance between the centroids of the two benzene caps of 9.143 Å (β distance) in the sulfate cryptate is slightly shorter than the 9.336 and 9.357 Å found in the I^- and $Cl_3(H_2O)_5$ cryptates, respectively. By contrast, in the corresponding deprotonated cryptand this distance is significantly reduced to 7.582 Å. Thus, these comparisons indicate that the 2,4,6-trialkylbenzene-capped hexaazacryptands have flexibility to enlarge their binding pockets, supplying enough room to accommodate large single anion or anions forming supramolecular entities.

In the crystal structure of $[(H_6xyl)(SO_4)(H_2O)_6](SO_4)_2\cdot 9.5H_2O$, six water molecules as well as one sulfate counterion are disordered over two positions (see below). This fact, associated with the water hydrogen atoms' absence (see below) in the final structure refinement, limited a complete analysis of the hydrogen bonding interactions. However, the crystal packing diagram shows that the five N–H hydrogen bonding sites, not involved in the molecular recognition of $(SO_4)(H_2O)_6$ participate with sulfate counter-anions and water molecules in an extensive network of N–H···O and O–H···O hydrogen bonds, at least with 1-D dimension.

Molecular mechanics and molecular dynamics calculations

The binding mode of sulfate and chloride by the H_6xyl^{6+} receptor was also investigated by means of molecular mechanics (MM) and molecular dynamics (MD) simulations using the Amber10[18] software with the GAFF force field.[19] No bond or angle terms were included in the calculations; consequently the attractive interactions between anions and the NH binding sites of H_6xyl^{6+} were primarily electrostatic.

The lowest energy conformations for H_6xyl^{6+} and its associations with SO_4^{2-} and Cl^- obtained in the gas phase through quenching molecular dynamics, as described in the experimental section, are shown in Fig. 8. The free protonated receptor "left view" exhibits a symmetric cage with a perfect C_3 symmetry axis, with α angles of 120° and a β distance of 9.138 Å. This conformation resembles the one found in the crystal structure, $[(H_6xyl)(SO_4)(H_2O)_6]^{4+}$. In contrast, the gas phase structure of $[(H_6xyl)(SO_4)]^{4+}$ does not have a C_3 symmetry, exhibiting α angles between 112.8 and 134.7° and a β distance of only 7.617 Å. The sulfate anion is in the middle of the cage at 3.875 Å from both 2,4,6-triethylbenzene caps and all four oxygen atoms are bound to N–H sites from different nitrogen centres, as shown in Fig. 8 (centre). All nitrogen centres are involved in the molecular recognition of the sulfate with H···O distances ranging from 1.79 to 1.99 Å. The structure of the association with chloride "right view" is also deprived of this symmetry, having α angles varying from 91.7 to 147.2° and a β distance of 8.355 Å. The chloride is inside the binding pocket, but it is only hydrogen bonded to three N–H sites with H···Cl distances of 2.12, 2.15 and 2.82 Å. These results indicate that the apparently rigid H_6xyl^{6+} has enough flexibility and space to accommodate anions with different binding requirements and sizes.

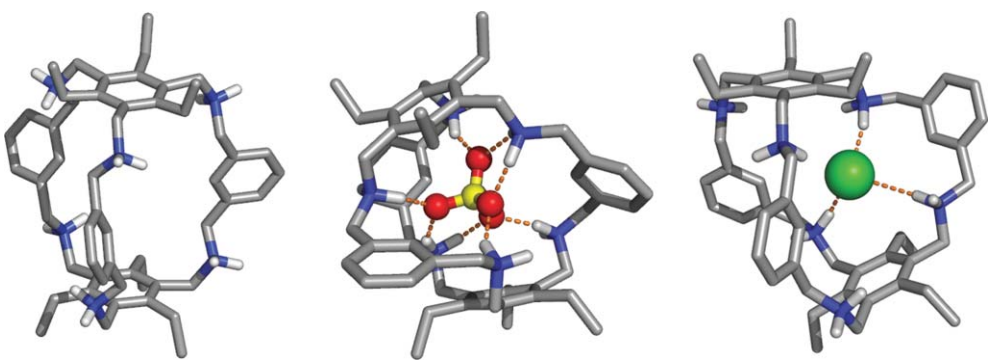

Fig. 8 Lowest energy conformations of H_6xyl^{6+} (left), $[(H_6xyl)(SO_4)]^{4+}$ (centre) and $[(H_6xyl)(Cl)]^{5+}$ (right) found in the conformational analyses. C–H hydrogen atoms have been omitted for clarity. The chloride atom is green and the hydrogen bonds are drawn as dashed orange lines. The colour scheme of the remaining atoms is given in Fig. 7.

The lowest energy structures found for $[(H_6xyl)(SO_4)]^{4+}$ and $[(H_6xyl)(Cl)]^{5+}$ associations were solvated with H_2O–MeOH (50 : 50 v/v), the solvent used in the potentiometric experiments. The dynamic behaviours of these two associations were investigated in this solvent *via* two independent MD runs carried out at 300 K for a long 15 ns using a NPT ensemble. The cage of the H_6xyl^{6+} receptor upon recognition of sulfate exhibits many different conformational shapes with the 2,4,6-triethylbenzene caps adopting different poses including an almost parallel arrangement comparable to that found in the $[(H_6xyl)(SO_4)(H_2O)_6]^{4+}$ crystal structure. These conformational changes are accompanied by variations in the cavity size-binding pocket with the distance between the two caps ($C_A \cdots C_A$ distance) ranging from 7.52 to 9.55 Å. The distance of the six nitrogen binding centres to the mass centre of H_6xyl^{6+}, defined by the atomic positions of these atoms ($N \cdots C_N$ distances), ranges between 3.22–5.84 Å, leading to corresponding average values of 4.43(33) Å. The evolution of the sulfate anion distance to the binding pocket centre ($S \cdots C_N$) along the MD simulations, plotted in Fig. 9 (left), indicates that the sulfate anion remains encapsulated during the entire course of the simulations, establishing with H_6xyl^{6+} weak and multiple exchangeable $N–H \cdots O$ binding interactions consistent with substantial variations of the receptor conformation accompanied by a significant anion movement into the cage. Indeed, occasionally the sulfate anion reaches the pocket boundaries, but never leaves the cage. These structural features are illustrated in Fig. 10 with two snapshots taken from the simulation.

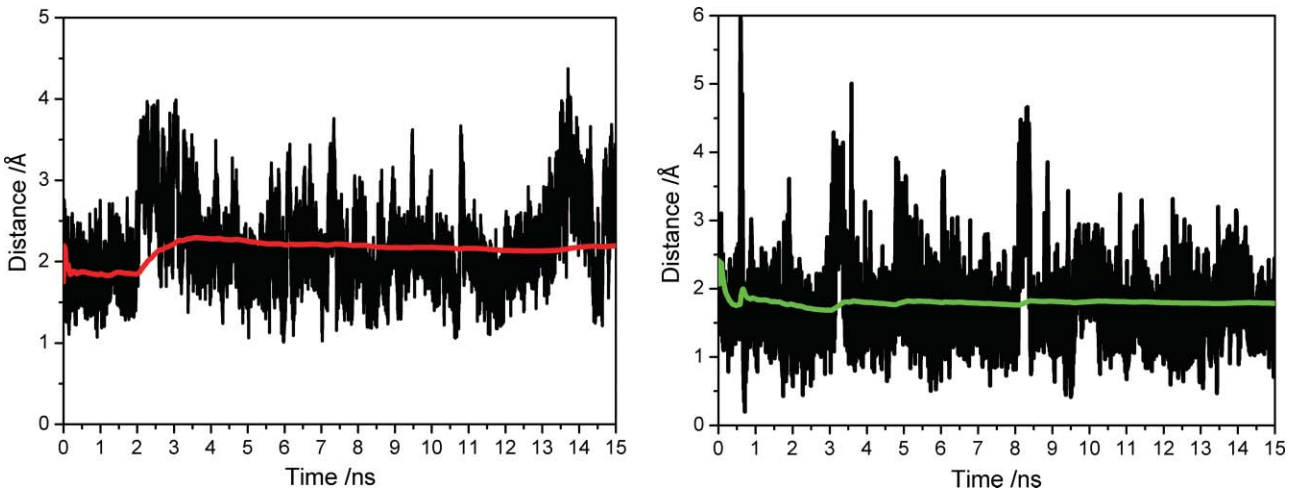

Fig. 9 Evolution of the sulfate (left) and chloride (right) distances to the binding pocket centre in H_2O–MeOH solution. The red and green lines correspond to the $S \cdots C_N$ and $Cl \cdots C_N$ accumulated average distances, respectively.

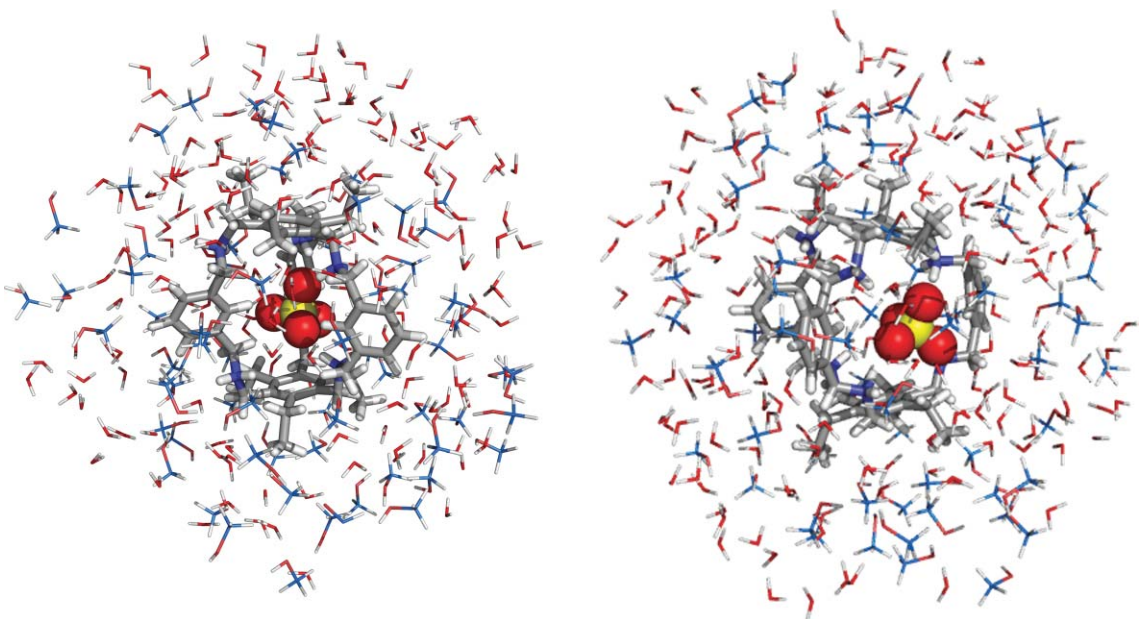

Fig. 10 Snapshots of $[(H_6xyl)(SO_4)]^{4+}$ taken at 6 ns (left) and 13.7 ns (right) of MD simulation, showing the anion located at the centre (left) and at the entrance (right) of the receptor pocket. Only the closest solvent molecules within 8 Å distance from H_6xyl^{6+} are shown. Colour scheme used as given in previous figures apart from the carbon atoms of MeOH, which are drawn in blue. The chloride counter-ions are omitted.

Table 3 Variations in N···X distances (Å) of $[(H_6xyl)(A)]^{n+}$ (A = SO_4^{2-}, n = 4; A = Cl^-, n = 5) over the MD simulations in H_2O–MeOH (50 : 50 v/v) solution at r.t.

Distances[a]	SO_4^{2-}[b]	Cl^-
$N_1 \cdots X$	4.48–8.99, 6.33(28)	3.00–6.04, 4.56(99)
$N_2 \cdots X$	4.23–8.98, 6.29(25)	3.05–5.95, 4.57(83)
$N_3 \cdots X$	3.06–6.62, 4.34(26)	3.10–5.86, 4.46(44)
$N_4 \cdots X$	3.08–6.62, 4.15(22)	3.17–5.89, 4.60(24)
$N_5 \cdots X$	3.02–6.34, 3.96(19)	2.98–5.89, 4.49(52)
$N_6 \cdots X$	3.11–6.29, 3.90(16)	3.22–6.05, 4.60(50)

[a] The range of distances is followed by the average distance with standard deviations calculated with N = 75 000. [b] X = S for the sulfate anion and X = Cl for the chloride anion.

Table 4 Variations in the number of water and methanol molecules enclosing the receptor and anion estimated with cut-off radii of 4.2 Å and 3.5 Å, respectively

Cryptate		Methanol[a]	Water[a]
$[(H_6xyl)(SO_4)]^{4+}$	$(H_6xyl)^{6+}$	0–16 (7)	7–30 (19)
	SO_4^{2-}	0–5 (1)	2–12 (7)
$[(H_6xyl)(Cl)]^{5+}$	$(H_6xyl)^{6+}$	0–17 (7)	7–33 (19)
	Cl^-	0–4 (1)	0–8 (3)

[a] In parentheses are the average numbers of solvent molecules.

The variations in the six S···N intermolecular distances reported during the course of simulations are listed in Table 3 together with the corresponding average values. Two S···N distances are much longer than the remaining four showing that the receptor recognizes the sulfate anion *via* only four NH_2 binding groups. Moreover, the plot of the S···N distances along the entire time of the simulation presented in Fig. S11 (see ESI†), indicates that the sulfate anion forms hydrogen bonds concomitantly with N–H groups from three or four nitrogen centres. Furthermore, all four sulfate oxygen atoms are involved in these interactions, with the N···O distances showing large variations between 2.47–7.86 Å, which indicates an exchange of the oxygen donors involved in the N–H···O hydrogen bonds.

Insights into the solvent effect on the anion recognition were obtained from the radial distributions (rdfs) of the O–H···C_N and O–H···O=S distances between the water or methanol molecules and the mass centres of the receptor and sulfate (defined by the four oxygen atoms), which are plotted in Fig. 11. The H_6xyl^{6+} presents a first water coordination shell centred at *ca.* 2.85 Å, while the anion exhibits three well defined water shells, the first one at 1.75 Å followed by the second and third ones at 2.95 Å and 3.75 Å, respectively. The water molecules solvate the receptor and the anion to a much higher extent than the methanol molecules, which form around the receptor and anion first coordination shells centred at 2.85 and 1.65 Å, respectively. This fact is consistent with the different numbers of water and methanol molecules that encompass the receptor and sulfate listed in Table 4. These numbers were calculated using cut-off distances of 4.2 Å and 3.5 Å from the receptor and anion mass centres, respectively, and therefore include the number of solvent molecules inside the pocket and hydrogen bonded to the anion.

The charge balance of $[(H_6xyl)(SO_4)]^{4+}$ in solution under periodic frontier conditions was achieved by the addition of four chloride anions. The Cl···C_N distances together with N···Cl distances found indicate that these counterions never enter into the binding pocket. In addition, as expected, some of the chloride counterions interact with N–H binding groups pointing towards the outside of the macrobicyclic cavity with the shortest N···Cl distances of 4.4 Å. Therefore, chloride counterions have a marginal effect on the dynamic behaviour of $[(H_6xyl)(SO_4)]^{4+}$ association.

As reported for the sulfate recognition, upon chloride binding the receptor also undergoes a large conformational change accompanied by wide variations in the $C_A \cdots C_A$, between 7.16 and 9.79 Å, and $C_N \cdots N$ distances from 3.00 to 6.05 Å for 15 ns of simulation. The evolution of the chloride anion distance to the binding pocket centre (Cl···C_N) during the course of simulation is also plotted in Fig. 9 (right). The chloride remains encapsulated in the binding pocket during almost the entire time of the simulation, leaving the receptor sporadically for a few picoseconds.

The wide variations found in all Cl···N intermolecular distances, listed in Table 3, indicate that all six nitrogen centres are involved in the anion binding with chloride swapping between them. It is also noteworthy that the chloride anion interacts

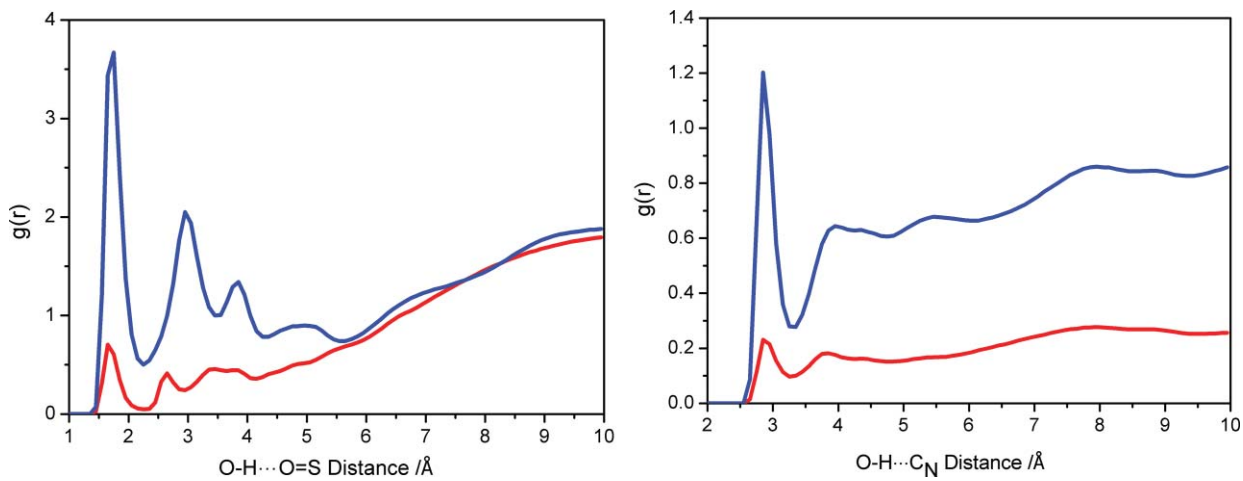

Fig. 11 Rdfs for O–H···O=S and O–H···C_N distances between the water (blue) and methanol (red) molecules and the centre of mass of the anion (left) and the receptor (right).

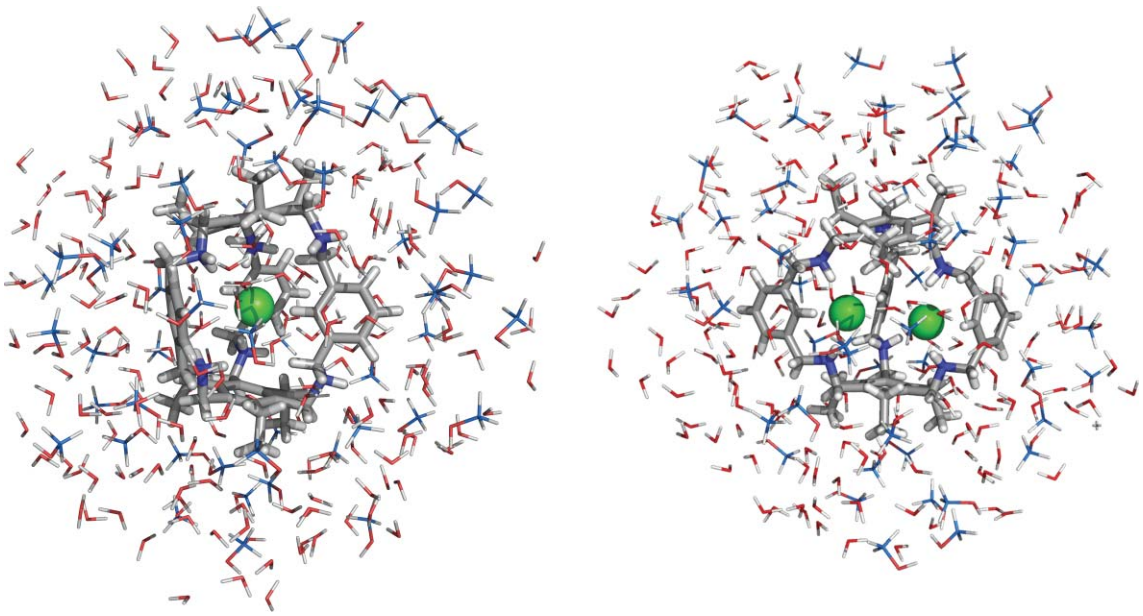

Fig. 12 Snapshots of the association between H_6xyl^{6+} and chloride taken at 3.0 ns (left) and 1.6 ns (right) of MD simulation showing one and two chloride anions accommodated in the cryptand cage. The remaining chloride anions are omitted. Remaining details as given in previous figures.

simultaneously with only two amine groups. In addition it occasionally shares the cage room with one of the five chloride counterions added to the periodic system for the charge balance of $[(H_6xyl)(Cl)]^{5+}$. These structural findings show that the receptor cage cavity is large enough to accommodate one or two chloride anions well. Fig. 12 presents two snapshots taken from the simulation showing one chloride inside the binding pocket and two chlorides accommodated in the receptor.

The rdfs for O–H $\cdots$ Cl and $C_N \cdots$ O–H distances presented in Fig. S12 (see ESI) once more show that the receptor and the chloride anion, are solvated to a much higher extent by the water than the methanol molecules, which is corroborated by the number of estimated solvent molecules that enclose both species in the H_2O–MeOH solvent mixture (Table 4).

In summary, the conventional MD simulations undertaken allowed a full understanding of the receptor binding preference for sulfate relative to chloride based on the structural findings reported.

Conclusions

Solution studies revealed that the receptor is remarkably selective for dinegative anions over mononegative ones at pH values below 5. In fact, in this pH region, the protonated receptor is able to exclusively bind any of the dinegative anions in the presence of equimolar amounts of all the mononegative ones. Therefore the receptor selectively uptakes sulfate in a mixture of sulfate and nitrate, making xyl an attractive candidate to be used in nuclear waste remediation.[4]

Sulfate, selenate and thiosulfate have the same charge, geometry and about the same size thus the receptor is unable to discriminate between them, a characteristic shared by most natural transporters.[20]

The potentiometric studies revealed that the main interactions are electrostatic in nature although contributions due to hydrogen bonding are not to be ruled out, as it was found that the poor hydrogen bond acceptor anions, I^- and ClO_4^-, have the lowest association constants. The importance of hydrogen bonds was also highlighted by the fact that when the receptor is fully protonated it lacks hydrogen bond acceptors for dihydrogen phosphate OH groups, which accounts for the low association constant found for $[(H_6xyl)(H_2PO_4)]^{5+}$, resembling the sulfate binding protein.[14] Single crystal X-ray studies showed that in the solid state one sulfate anion is encapsulated into the receptor cage through three N–H $\cdots$ O hydrogen bonding interactions. The molecular recognition process was investigated in solution theoretically by MD simulations, which also indicated that the sulfate and chloride binding is dictated by electrostatic interactions complemented by multiple N–H $\cdots$ O or N–H $\cdots$ Cl hydrogen bonds. MD simulations allowed an understanding of the receptor binding preference for sulfate relative to chloride.

Experimental

All solvents and chemicals were commercially purchased of reagent grade quality and used as supplied without further purification, except 1,3,5-tris(aminomethyl)-2,4,6-triethylbenzene which was prepared according to literature methods.[21] Potassium or sodium salts of the anions were purchased as analytical grade and were used without further purification. *p*-Toluenesulfonic acid (HTsO) was purchased from Aldrich, and potassium *p*-toluenesulfonate (KTsO) was prepared by the neutralization of HTsO with KOH in water, followed by recrystallisation from H_2O–MeOH. All the solutions were prepared using demineralised water (obtained by a Millipore/Milli-Q system) and methanol purified by standard methods.[22] NMR spectra used for characterization of products and binding experiments were recorded on a Bruker Avance 400 instrument. The reference used for the ^{1}H NMR measurements in $CDCl_3$ was TMS and in D_2O the 3-(trimethylsilyl)propanoic acid-d_4-sodium salt. Peak assignments

are based on peak integration and multiplicity for 1-D ^{1}H spectra and on COSY, NOESY and HMQC experiments. Microanalyses were carried out by the ITQB Microanalytical Service.

Synthesis

Schiff base of xyl. A solution of 1,3,5-tris(aminomethyl)-2,4,6-triethylbenzene (300 mg, 1.2 mmol) in MeCN (30 cm^{-3}) was added dropwise over 15 min to a magnetically stirred solution of isophthaldehyde (242 mg, 1.8 mmol) in MeCN (30 cm^{-3}). The mixture was left stirring overnight and a white precipitate formed which was separated by filtration and washed with MeCN (about 100 cm^{-3}) to remove any unreacted starting materials. The precipitate was suspended in $CHCl_3$ (100 cm^{-3}), ultrasonicated for 1 h and filtered. Evaporation of the solvent yielded the desired hexaimine (432 mg, 90%) which was dried in a vacuum. δ_H (400 MHz; $CDCl_3$; 25 °C; Me_4Si) 1.15 (18 H, t, *J* 8.0 Hz, $BzCH_2CH_3$), 2.25 (12 H, q, *J* 8.0 Hz, $BzCH_2CH_3$), 5.01 (12 H, s, CH_2Bz), 6.99 (3 H, s, H2, *m*-xylyl), 7.42 (3 H, t, *J* 7.6 Hz, H5, *m*-xylyl), 7.72 (6 H, s, HC=N) and 8.08 ppm (6 H, d, *J* 8.0 Hz, H4, H6, *m*-xylyl); δ_C (100 MHz; $CDCl_3$; 25 °C; Me_4Si) 16.11 ppm ($BzCH_2CH_3$), 23.70 ($BzCH_2CH_3$), 54.82 (CH_2Bz), 128.68 (C6, C4, *m*-xylyl), 129.42 (C5, *m*-xylyl), 130.71 (C2, *m*-xylyl), 131.36 (C2, C4, C6, Bz), 136.80 (C1, C3, *m*-xylyl), 144.41 (C1, C3, C5, Bz) and 157.95 ppm (C=N).

xyl. Solid $NaBH_4$ (1.226 g, 32.4 mmol) was added in small portions to a magnetically stirred suspension of the hexaimine (432 mg, 0.54 mmol) in methanol (65 cm^{-3}). After the addition was completed, the mixture was left stirring at room temperature for two hours, and under reflux overnight. The solution was evaporated under vacuum almost to dryness, then 1 mol dm^{-3} HCl (10 cm^{-3}) was added and the entire methanol was evaporated. The solution was made strongly basic with 6 mol dm^{-3} KOH and extracted with $CHCl_3$ (3 × 50 cm^{-3}). The organic portions were collected in an Erlenmeyer flask, dried over anhydrous sodium sulfate, filtered and evaporated to dryness to give xyl (351 mg, 80%) as a colorless oil which when dried under vacuum gave a white solid. Mp 146 °C (decomp.); found: C, 69.85; H, 8.3; N, 8.8. Calc. for $C_{54}H_{72}N_6{\cdot}CHCl_3{\cdot}H_2O$: C, 70.1; H, 8.0; N, 8.9%; δ_H (400 MHz; $CDCl_3$; 25 °C; Me_4Si) 1.18 (18 H, t, *J* 8.0 Hz, $BzCH_2CH_3$), 1.35 (br s, NH + H_2O), 2.70 (12 H, q, *J* 8.0 Hz, $BzCH_2CH_3$), 3.76 (12 H, s, CH_2Bz), 3.89 (12 H, s, *m*-xylyl-CH_2), 7.01 (6 H, d, *J* 8.0, H6, H4, *m*-xylyl), 7.14 (3 H, t, *J* 4.0, H5, *m*-xylyl) and 7.26 ppm (3 H, s, H2, *m*-xylyl); δ_C (100 MHz; $CDCl_3$; 25 °C; Me_4Si) 15.63 ppm ($BzCH_2CH_3$), 21.70 ($BzCH_2CH_3$), 47.37 (CH_2Bz), 54.01 (*m*-xylyl-CH_2), 122.23 (C2, *m*-xylyl), 124.72 (C4, C6, *m*-xylyl), 126.55 (C5, *m*-xylyl), 133.15 (C2, C4, C6, Bz), 139.87 (C1, C3, *m*-xylyl) and 141.37 ppm (C1, C3, C5, Bz); *m*/*z* (ESI-MS; MeOH) 805.6 $[M + H]^+$, 403.3 $[M + 2H]^{2+}$.

Crystals of $[(H_6xyl)(SO_4)(H_2O)_6](SO_4)_2{\cdot}9.5H_2O$

xyl (4.03 mg, 5 μmol) was dissolved in acetone (500 μL) and 97% H_2SO_4 (0.833 μL) was added. Immediately a white precipitate was formed. Water (140 μL) was added and the solution heated until it was clear, then the mixture was allowed to slowly cool to r.t. Single colourless crystals suitable for X-ray crystallography were obtained overnight.

Potentiometric measurements

Reagents and solutions. All solutions were prepared in water–methanol (50 : 50 v/v) mixed solvent. A stock solution of the receptor was prepared at *ca*. 1.5×10^{-3} mol dm^{-3}. Anion solutions were prepared at 0.1 mol dm^{-3} from the corresponding potassium salts and the concentrations were checked by titration with standard 0.1 mol dm^{-3} KOH solutions. Carbonate-free solutions of the KOH titrant were prepared from a Merck ampoule diluted with 500 cm^{-3} of water (freshly boiled for about 2 h and allowed to cool under nitrogen) to which 500 cm^{-3} of methanol was added. These solutions were discarded every time the carbonate concentration was about 0.5% of the total amount of base. The titrant solutions were standardized (tested by Gran's method).[23]

Equipment and working conditions. The potentiometric setup consisted of a 50 cm^3 glass-jacketed titration cell sealed from the atmosphere and connected to a separate glass-jacketed reference electrode cell by a salt bridge containing 0.10 mol dm^{-3} KTsO solution. An Orion 720A measuring instrument fitted with a Metrohm 6.0150.100 glass electrode and a Mettler Toledo InLab 301 Ag/AgCl reference electrode was used for the measurements. The ionic strength of the experimental solutions was kept at 0.10 ± 0.01 mol dm^{-3} with KTsO, the temperature was controlled at 298.2 ± 0.1 K using a Huber Polystat cc1 thermostatic system and atmospheric CO_2 was excluded from the titration cell during experiments by passing purified nitrogen across the top of the experimental solution. Titrant solutions were added through capillary tips at the surface of the experimental solution by a Metrohm Dosimat 665 automatic burette. The titration procedure was automatically controlled by software after selection of suitable parameters. The glass electrode was pre-treated by soaking it in the water–methanol (50 : 50 v/v) solution over a period of 2 days, in order to prevent erratic responses.

Measurements. The $[H^+]$ of the solutions was determined by the measurement of the electromotive force of the cell, $E = E'^{\circ} + Q\log[H^+] + E_j$. The term pH is defined as $-\log[H^+]$. E'°, Q, E_j and K'_w were determined by titration of a solution of known hydrogen-ion concentration at the same ionic strength, using the acid pH range of the titration. The liquid-junction potential, E_j, was found to be negligible under the experimental conditions used. The value of K'_w was determined from data obtained in the alkaline range of the titration, considering E'° and Q valid for the entire pH range and found to be equal to $10^{-13.91}$ in our experimental conditions. Before and after each set of titrations the glass electrode was calibrated as a $[H^+]$ probe by titration of a 1.0×10^{-3} mol dm^{-3} standard HCl solution with standard KOH. The potentiometric equilibrium measurements were carried out using 20.00 cm^3 of ≈1.50×10^{-3} mol dm^{-3} ligand solution diluted to a final volume of 30.00 cm^3, in the absence of any anions, then in the presence of each anion at 1 : 3 R : A ratios (R = receptor and A = anion). Care has been taken to maintain unaltered the methanol–water ratio in measured solution. The exact amount of ligand was obtained by determination of the excess of acid present in a mixture of xyl and standard *p*-toluenesulfonic acid 1.0×10^{-2} mol dm^{-3} by titration with standard KOH solution.

Calculation of equilibrium constants. Overall protonation constants, β_i^H, of both ligand and anions, were calculated by fitting the potentiometric data obtained for all the performed titrations

in the same experimental conditions with the HYPERQUAD program.[24] All these constants were taken as fixed values to obtain the equilibrium constants of the new species from the experimental data corresponding to all the titrations at 1 : 3 R : A ratio, also using the HYPERQUAD program. The initial computations were obtained in the form of overall stability constants, $\beta_{H_hL_lA_a}$ values, $\beta_{H_hL_lA_a} = [H_hL_lA_a]/[H]^h[L]^l[A]^a$. The errors quoted are the standard deviations of the overall association constants given directly by the program for the input data, which include all the experimental points of all titration curves. The HYSS program[25] was used to calculate the concentration of equilibrium species from the calculated constants from which distribution diagrams were plotted. The species considered in a particular model were those that could be justified by the principles of supramolecular chemistry.

NMR studies

^{1}H-NMR of the cryptates. Solutions of $(H_6xyl)(TsO)_6$ and respective cryptates where prepared in D_2O ($\approx 2.0 \times 10^{-3}$ mol dm^{-3}) and the pD was adjusted to 3.80 by addition of DTsO or KOD with an Orion 420A instrument fitted with a combined Ingold 405M3 microelectrode. The pH*, the reading of the pH meter previously calibrated with two standard aqueous buffers at pH 4 and 8, was measured directly in the NMR tube. The final pD was calculated from pD = pH* + (0.40 ± 0.02).[26]

Job's plots. Stock solutions of 2.0×10^{-3} mol dm^{-3} $(H_6xyl)(TsO)_6$ and K_2SO_4 were prepared in D_2O. Ten NMR tubes were prepared having a total concentration of $(H_6xyl)(TsO)_6$ and of K_2SO_4 maintained at 2.0×10^{-3} mol dm^{-3}. The pD value was adjusted to 3.80 with DTsO or KOD. The chemical shift changes for each solution were measured, and the product of the increment in chemical shift and receptor concentration *versus* the molar fraction of the receptor was plotted. A curve was generated where the maximum point indicated the stoichiometry of the association by use of the equation: $[C] = [R]_0 \times (\delta_{obs} - \delta_R)/(\delta_{max} - \delta_R)$, where $[R]_0$ is the total receptor concentration, δ_{obs} is the observed chemical shift, δ_R is the chemical shift of the free receptor, and δ_{max} is the chemical shift of the cryptate. Because $\delta_{max} - \delta_R$ is a constant, the concentration of the associated entity is proportional to $\Delta\delta \times [R]_0$ (where $\Delta\delta = \delta_{obs} - \delta_R$). Plots of $\Delta\delta X_R$ as a function of X_R (where X_R is the molar fraction of the receptor) that exhibit a maximum at $X_R = 0.5$, indicate a 1 : 1 association.

Mass spectrometry studies

Two solutions were prepared, one containing $(H_6xyl)(TsO)_6$ and K_2SO_4 diluted to a concentration of 1×10^{-5} mol dm^{-3} in water–methanol (50 : 50 v/v) and another containing $(H_6xyl)(TsO)_6$, K_2SO_4 and KNO_3 diluted to a concentration of 1×10^{-5} mol dm^{-3} also in water–methanol (50 : 50 v/v). Mass spectra for both solutions have been acquired in the positive polarity mode, after their direct injection into the mass spectrometer using a syringe pump, in a Bruker Daltonics Esquire 3000plus mass spectrometer equipped with an ESI source. The following tuned conditions were used: ion spray voltage, 30–80 V ramp range capillary exit and temperature of the heated capillary, 100 °C. Nitrogen was used as a drying gas at a flow rate of 5 L min^{-1} and at a constant pressure of 15 psi.

Crystallography

Crystal data of $[(H_6xyl)(SO_4)(H_2O)_6](SO_4)_2 \cdot 9.5H_2O$. Mr = 1378.65. Triclinic, space group $P\bar{1}$, $Z = 2$, $a = 12.5490(5)$, $b = 15.0384(6)$, $c = 19.0959(7)$ Å, $\alpha = 99.510(2)$, $\beta = 99.578(2)$, $\gamma = 98.598(2)°$, $V = 3446.1(2)$ Å^3, ρ(calc) = 1.329 Mg m^{-3}, 0.191 mm^{-1}. 55623 reflections were collected and subsequently merged to 16070 unique reflections with an R_{int} of 0.0365.

The single crystal X-ray data were collected on a CCD Bruker APEX II at 150(2) K using graphite monochromatized Mo-Kα radiation ($\lambda = 0.71073$ Å). The crystal of the complex was positioned at 40 mm from the CCD and the spots were measured using a counting time of 120 s. Data reduction including a multi-scan absorption correction was carried out using the SAINT-NT from Bruker AXS. The structure was solved by direct methods and by subsequent difference Fourier syntheses and refined by full matrix least squares on F^2 using the SHELX-97 suite.[27] One SO_4^{2-} counterion was found to be disordered with the sulfur and four oxygen atoms occupying two alternative positions, which were included in the model refinement with refined occupancies of x and $1 - x$, x being equal to 0.592(4). Furthermore, the S–O distances of this anion were restrained to 1.54 Å. Among sixteen water of crystallization solvent molecules, six were found to be disordered over two or three positions (one molecule), with occupation factors ranging from 0.25 to 0.75. In addition, one water molecule occupying a single position was refined with an occupation factor set to 0.5. Anisotropic thermal parameters were used for all non-hydrogen atoms. The N–H and C–H hydrogen atoms were refined with $U_{iso} = 1.2U_{eq}$ of the parent atom. The hydrogen atoms of the water molecules were not apparent from the last Fourier difference maps and they were not included in the structure refinement.

The final refinement of 935 parameters converged to final R and R_w indices $R_1 = 0.0761$ and w$R_2 = 0.2188$ for 10951 reflections with $I > 2\sigma(I)$ and $R_1 = 0.1114$ and w$R_2 = 0.2510$ for all hkl data.

Molecular modelling simulations

MM and MD simulations were carried out using the Amber10[18] suite of programs, with parameters for the receptor and sulfate taken from the GAFF[19] force field. The methanol solvent molecules were described using a full atom solvent model with atomic charges and force field parameters taken from ref. 28 and the TIP3P model was used for the water.[29] The chloride ion with a charge of −1 was described with van der Waals parameters taken from ref. 30. The atomic charges for the receptor and sulfate anion were calculated at the HF/6-31G* level using RESP methodology with Gaussian03.[31]

The structure of the protonated receptor was taken from the crystal structure of $[(H_6xyl)(SO_4)(H_2O)_6](SO_4)_2 \cdot 9.5H_2O$. The conformational analysis of H_6xyl^{6+} was carried out by MD using the following procedure: the MM minimized structure was subjected to a MD quenching run in the gas phase at 2000 K using a time step of 1 fs. 20 000 conformations were collected over 2 ns simulation time and then they were minimized by MM using an in-house script.

The docking between the receptor and sulfate and chloride anions was also performed through quenching molecular dynamics using an equivalent procedure adopted for the receptor. The anion

was located inside the receptor cavity and 50 000 conformations were collected over 5 ns simulation.

The lowest energy geometric arrangements found for sulfate and chloride associations were immersed in H_2O–MeOH cubic boxes having a total of 2905 solvent molecules. The electrostatic neutrality of the periodic cubic systems was achieved with the replacement of solvent molecules by the equivalent number of chloride anions depending on the total charge of the system.

All the MD simulations started with equilibration of the system under periodic boundary conditions using a multistage protocol composed of two successive MM minimizations, to eliminate undesired short potential contacts. In the first MM minimization 10 000 steps of steepest descent method followed by 10 000 steps of conjugate gradient methods was done keeping a positional restrain of 500 kcal mol^{-1} $Å^{-2}$ on the associations. In the second MM minimization the positional restrain was removed and 1000 steps by the steepest descent method followed by 10 000 steps by conjugate gradient methods were made. Next, a MD-NVT simulation with a weak positional restrain of 10 kcal mol^{-1} $Å^{-2}$ on the associations was run for 50 ps to bring the temperature to 300 K. Then, the positional restrain was removed and the equilibration process proceeded with a MD-NPT simulation run of 500 ps to adjust the solvent density giving rise to cubic boxes with final sizes between 38.9 and 40.0 Å. At this stage the average value of the density remained constant at least during the last 100 ps of the NPT simulation and in agreement with the experimental density at r.t. for H_2O–MeOH (50 : 50 v/v). Finally, a MD data collection run was produced at 300 K and 1 atm for 15 ns using a NPT assemble. All the bonds involving hydrogen atoms were constrained using SHAKE,[32] which allowed the use of a time step of 2 fs. The particle mesh Ewald method[33] was used to describe long range electrostatic interactions and the non-bonded van der Waals interactions were subjected to a 12 Å cut-off.

Acknowledgements

The authors acknowledge FCT and POCI, with co-participation of the European Community funds FEDER, for financial support under projects PTDC/QUI/56569/2004 and PTDC/QUI/68582/2006. The NMR spectrometers are part of the National NMR Network and were acquired with funds from FCT and FEDER. We also acknowledge M. C. Almeida for providing elemental analysis and ESI-MS data from the Elemental Analysis and Mass Spectrometry Service at the ITQB. Pedro Mateus and Sílvia Carvalho thank FCT for the grants, SFRH/BD/36159/2007 and SFRH/BPD/42357/2007, respectively.

References

1 (*a*) Anion Coordination Chemistry II, ed. P. A. Gale, *Coord. Chem. Rev*, 2006, **250**, 2917–3244; (*b*) 35 years of Synthetic Anion Receptor Chemistry, ed. P. A. Gale, *Coord. Chem. Rev.*, 2003, **240**, 1–226; (*c*) J. L. Sessler, P. I. Sansom, A. Andrievsky and V. Kral, in *Supramolecular Chemistry of Anions*, ed. A. Bianchi, K. Bowman-James and E. Garcia-España, Wiley-VCH, NY, 1997, pp. 355–419.
2 D. N. Sheppard and M. J. Welsh, *Physiol. Rev.*, 1999, **79**, 23–45.
3 (*a*) M. Brunetti, L. Terracina, L. Timio, P. Saronio and E. Capodicasa, *J. Nephrol.*, 2001, **14**, 27–31; (*b*) I. Fernandes, D. Laouari, P. Tutt, G. Hampson, G. Friedlander and C. Silve, *Kidney Int.*, 2001, **59**, 210–221.
4 B. A. Moyer, L. H. Delmau, C. J. Fowler, A. Ruas, D. A. Bostick, J. L. Sessler, E. Katayev, G. D. Pantos, J. M. Llinares, M. A. Hossain, S. O. Kang, and K. Bowman-James, in Template Effects and Molecular Organization, ed. R. van Eldik and K. Bowman-James, Elsevier, Oxford, *Adv. Inorg. Chem.*, 2007, **59**, 175–204.
5 (*a*) V. McKee, J. Nelson and R. M. Town, *Chem. Soc. Rev.*, 2003, **32**, 309–325, and references therein; (*b*) R. J. Motekaitis, A. E. Martell, J.-M. Lehn and E.-I. Watanabe, *Inorg. Chem.*, 1982, **21**, 4253–4251; (*c*) R. J. Motekaitis, A. E. Martell, I. Murase, J.-M. Lehn and M. W. Hosseini, *Inorg. Chem.*, 1988, **27**, 3630–3636; (*d*) S. Mason, J. M. Llinares, M. Morton, T. Clifford and K. Bowman-James, *J. Am. Chem. Soc.*, 2000, **122**, 1814–1815; (*e*) J. Aguilar, T. Clifford, A. Danby, J. M. Llinares, S. Mason, E. Garcia-España and K. Bowman-James, *Supramol. Chem.*, 2001, **13**, 405–417; (*f*) J. Nelson, M. Nieuwenhuyzen, I. Pál and R. M. Town, *Dalton Trans.*, 2004, 2303–2308.
6 K. Gloe, H. Stephan and M. Grotjahn, *Chem. Eng. Technol.*, 2003, **26**, 1107–1117.
7 D. Heyer and J.-M. Lehn, *Tetrahedron Lett.*, 1986, **27**, 5869–5872.
8 O. Francesconi, A. Ienco, G. Moneti, C. Nativi and S. Roelens, *Angew. Chem., Int. Ed.*, 2006, **45**, 6693–6696.
9 M. Arunachalam, I. Ravikumar and P. Ghosh, *J. Org. Chem.*, 2008, **73**, 9144–9147.
10 D. Chen and A. E. Martell, *Tetrahedron*, 1991, **47**, 6895–6902.
11 G. Hennrich and E. V. Anslyn, *Chem.–Eur. J.*, 2002, **8**, 2218–2224.
12 (*a*) B. Dietrich, J. Guilhem, J.-M. Lehn, C. Pascard and E. Sonveau, *Helv. Chim. Acta*, 1984, **67**, 91–104; (*b*) M. J. Hynes, B. Maubert, V. McKee, R. M. Town and J. Nelson, *J. Chem. Soc., Dalton Trans.*, 2000, 2853–2859; (*c*) T. Clifford, A. Danby, J. M. Llinares, S. Mason, N. W. Alcock, D. Powell, J. A. Aguilar, E. Garcia-España and K. Bowman-James, *Inorg. Chem.*, 2001, **40**, 4710–4720.
13 M. T. Albelda, M. A. Bernardo, E. Garcia-España, M. L. Godino-Salido, S. V. Luis, M. J. Melo, F. Pina and C. Soriano, *J. Chem. Soc., Perkin Trans. 2*, 1999, 2545–2549.
14 B. L. Jacobson and F. A. Quiocho, *J. Mol. Biol.*, 1988, **204**, 783–787.
15 B. M. Maubert, J. Nelson, V. McKee, R. M. Town and I. Pál, *J. Chem. Soc., Dalton Trans.*, 2001, 1395–1397.
16 A. Bianchi and E. Garcia-España, *J. Chem. Educ.*, 1999, **76**, 1727–1732.
17 K. Hirose, *J. Inclusion Phenom. Macrocyclic Chem.*, 2001, **39**, 193–209.
18 D. A. Case, T. A. Darden, T. E. Cheatham III, C. L. Simmerling, J. Wang, R. E. Duke, R. Luo, M. Crowley, R. C. Walker, W. Zhang, K. M. Merz, B. Wang, S. Hayik, A. Roitberg, G. Seabra, I. Kolossváry, K. F. Wong, F. Paesani, J. Vanicek, X. Wu, S. R. Brozell, T. Steinbrecher, H. Gohlke, L. Yang, C. Tan, J. Mongan, V. Hornak, G. Cui, D. H. Mathews, M. G. Seetin, C. Sagui, V. Babin, P. A. Kollman, *AMBER 10*, University of California, San Francisco, 2008.
19 J. Wang, R. M. Wolf, J. W. Caldwell, P. A. Kollmann and D. A. Case, *J. Comput. Chem.*, 2004, **25**, 1157–1174.
20 D. Markovich, *Physiol. Rev.*, 2001, **81**, 1499–1533.
21 K. J. Wallace, R. Hanes, E. V. Anslyn, J. Morey, K. V. Kilway and J. Siegel, *Synthesis*, 2005, 2080–2083.
22 D. D. Perrin and W. L. F. Armarego, *Purification of Laboratory Chemicals*, Pergamon, Oxford, 3rd edn, 1988, p. 217.
23 F. J. Rossotti and H. J. Rossotti, *J. Chem. Educ.*, 1965, **42**, 375–378.
24 P. Gans, A. Sabatini and A. Vacca, *Talanta*, 1996, **43**, 1739–1753.
25 L. Alderighi, P. Gans, A. Ienco, D. Peters, A. Sabatini and A. Vacca, *Coord. Chem. Rev.*, 1999, **184**, 311–318.
26 R. Delgado, J. J. R. F. da Silva, M. T. S. Amorim, M. F. Cabral, S. Chaves and J. Costa, *Anal. Chim. Acta*, 1991, **245**, 271–282.
27 G. M. Sheldrick, *Acta Crystallogr., Sect. A: Found. Crystallogr.*, 2008, **64**, 112.
28 J. W. Caldwell and P. A. Kollman, *J. Phys. Chem.*, 1995, **99**, 6208–6219.
29 W. L. Jorgensen, J. Chandrasekhar, J. D. Madura, R. W. Impey and M. L. Klein, *J. Chem. Phys.*, 1983, **79**, 926–935.
30 I. S. Joung and T. E. Cheatham III, *J. Phys. Chem. B*, 2008, **112**, 9020–9041.
31 M. J. Frisch, G. W. Trucks, H. B. Schlegel, G. E. Scuseria, M. A. Robb, J. R. Cheeseman, J. A. Montgomery, Jr., T. Vreven, K. N. Kudin, J. C. Burant, J. M. Millam, S. S. Iyengar, J. Tomasi, V. Barone, B. Mennucci, M. Cossi, G. Scalmani, N. Rega, G. A. Petersson, H. Nakatsuji, M. Hada, M. Ehara, K. Toyota, R. Fukuda, J. Hasegawa, M. Ishida, T. Nakajima, Y. Honda, O. Kitao, H. Nakai, M. Klene, X. Li, J. E. Knox, H. P. Hratchian, J. B. Cross, V. Bakken, C. Adamo, J. Jaramillo,

R. Gomperts, R. E. Stratmann, O. Yazyev, A. J. Austin, R. Cammi, C. Pomelli, J. Ochterski, P. Y. Ayala, K. Morokuma, G. A. Voth, P. Salvador, J. J. Dannenberg, V. G. Zakrzewski, S. Dapprich, A. D. Daniels, M. C. Strain, O. Farkas, D. K. Malick, A. D. Rabuck, K. Raghavachari, J. B. Foresman, J. V. Ortiz, Q. Cui, A. G. Baboul, S. Clifford, J. Cioslowski, B. B. Stefanov, G. Liu, A. Liashenko, P. Piskorz, I. Komaromi, R. L. Martin, D. J. Fox, T. Keith, M. A. Al-Laham, C. Y. Peng, A. Nanayakkara, M. Challacombe, P. M. W. Gill, B. G. Johnson, W. Chen, M. W. Wong, C. Gonzalez and J. A. Pople, *GAUSSIAN 03 (Revision C.2)*, Gaussian, Inc., Wallingford, CT, 2004.

32 J. P. Ryckaert, G. Cicotti and H. J. C. Berendsen, *J. Comput. Phys.*, 1977, **23**, 327–341.

33 U. Essmann, L. Perera, M. L. Berkowitz, T. Darden, H. Lee and L. G. Perdensen, *J. Chem. Phys.*, 1995, **103**, 8577–8593.